Available online at www.sciencedirect.com
ScienceDirect
Continental Shelf Research 27 (2007) 713–728
CONTINENTAL SHELF RESEARCH
www.elsevier.com/locate/csr

Modelling offshore sand wave evolution

A.A. Németh[a,*,1], S.J.M.H. Hulscher[b], R.M.J. Van Damme[c]

[a]*Witteveen + Bos Consulting Engineers, P.O. Box 233, 7400 AE Deventer, The Netherlands*
[b]*Department of Civil Engineering, University of Twente, P.O. Box 217, 7500 AE Enschede, The Netherlands*
[c]*Department of Applied Mathematics, University of Twente, P.O. Box 217, 7500 AE Enschede, The Netherlands*

Received 23 December 2005; received in revised form 6 November 2006; accepted 14 November 2006
Available online 22 January 2007

Abstract

We present a two-dimensional vertical (2DV) flow and morphological numerical model describing the behaviour of offshore sand waves. The model contains the 2DV shallow water equations, with a free water surface and a general bed load formula. The water movement is coupled to the sediment transport equation by a seabed evolution equation. Using this model, we investigate the evolution of sand waves in a marine environment. As a result, we find sand wave saturation for heights of 10–30% of the average water depth on a timescale of decades. The stabilization mechanism, causing sand waves to saturate, is found to be based on the balance between the shear stress at the seabed and the principle that sediment is transported more easily downhill than uphill. The migration rate of the sand waves decreases slightly during their evolution. For a unidirectional steady flow the sand waves become asymmetrical in the horizontal direction and for a unidirectional block current asymmetrical in the vertical. A sensitivity analysis showed the slope effect of the sediment transport plays an important role herein. Furthermore, the magnitude of the resistance at the seabed and the eddy viscosity influence both the timescale and height of sand waves. The order of magnitudes found of the time and spatial scales coincide with observations made in the southern bight of the North Sea, Japan and Spain.

Keywords: Numerical analysis; Finite amplitude waves; Sand waves; Shelf seas

1. Introduction

Offshore sand waves are large scale rhythmic bed features having typical wavelengths of several hundreds of meters and can be found in shallow seas such as the North Sea. Their crests are oriented more or less perpendicular to the principal direction of the current (Hulscher, 1996). The heights, the vertical distance between crest and trough, of sand waves can grow up to 30% of the average water depth. Therefore, the relative sand wave height can be considered as significant.

Insight into the behaviour of these sand waves is crucial to enable cost-effective management practices. Due to the large height of sand waves compared to the water depth in combination with the timescale of years on which they are assumed to be active, they play an important role in navigation in coastal seas (Németh et al., 2003).

Knaapen and Hulscher (2002) developed an evolution model based on data assimilation and

*Corresponding author.
E-mail address: a.nemeth@witteveenbos.nl (A.A. Németh).
[1]Previously at Department of Civil Engineering, University of Twente, P.O. Box 217, 7500 AE Enschede, The Netherlands.

0278-4343/$ - see front matter © 2006 Elsevier Ltd. All rights reserved.
doi:10.1016/j.csr.2006.11.010

investigated data sets of a field of sand waves near Japan. This analysis showed that when a sand wave is dredged, it is able to recover on a timescale of about eight years. Morelissen et al. (2003) extended this model by allowing sand waves to migrate using a modified Landau equation. Despite the success of this empirical method, it does not include the full knowledge of sand wave physics, as the physical basis was lacking at that moment. Therefore, it cannot facilitate the investigation of the mechanisms leading to nonlinear sand wave behaviour.

Based on Huthnace (1982a,b), Hulscher (1996), Gerkema (2000) and Komarova and Hulscher (2000), Németh et al. (2002) developed a model describing the formation and migration of infinitely small-amplitude sand waves based on a stability analysis. The model uses a combination of periodic and steady water motion. It gives insight into the initial evolution and migration of sand waves assuming they are free instabilities of the seabed water system.

Komarova and Newell (2000) investigated the model by Hulscher (1996) combined with the time-dependent viscosity parameterization from Komarova and Hulscher (2000) using a weakly nonlinear analysis. This analysis led to coupled spatial variations of sand waves and the average bed level, of which the latter shows similarities with tidal sandbanks. However, sand wave migration was not investigated in this analysis.

In addition to the research on offshore sand waves, several authors investigated similar bed forms in a unidirectional flow setting in rivers using numerical methods. Johns et al. (1990) and Stansby and Zhou (1998) discussed unidirectional steady water movement over dune-like features with steep slopes. The focus of that work is on flow separation, which we do not expect for offshore sand waves with a smaller steepness than dunes found in rivers. Fredsøe and Deigaard (1992) discuss the behaviour of sand waves based on a model describing fully-developed sand dunes in rivers (see also a.o. Hansen, 1989). Sand waves under the influence of oscillatory water movement are schematized as bed forms formed under the influence of a unidirectional steady current, with a modification for the reversing current. Therefore, periodic water motion is not taken directly into account. Furthermore, the model does not describe bed form evolution. Richards and Taylor (1981) discussed flow and sediment transport characteristics for more sandwave-like bed forms in a unidirectional steady flow, with milder slopes than river dunes. In addition, they discuss the response of the seabed for various shapes of the sand wave. For a detailed discussion on differences and similarities between river dunes and sand waves we refer to Hulscher and Dohmen-Janssen (2005). Idier (2003) investigated sinusoidal sand waves for various amplitudes with a numerical model for unidirectional steady flow conditions.

Assuming sand waves to be free instabilities of the seabed–water system, we understand the initial instability mechanism apart from minor aspects. However, the intermediate term behaviour of offshore sand waves (especially for periodic water motion) is still not fully understood. Here, we are interested in the evolution of sand waves and their stabilization processes, together with their maximum height.

In Németh et al. (2006), a numerical simulation model has been developed and validated mathematically with the help of the linear stability analysis discussed in Németh et al. (2002). This simulation model enables the description of the entire evolutionary process of sand waves.

Here, we investigate the behaviour of sand waves having finite dimensions in order to investigate the mechanisms determining the stabilization of the evolution of sand waves and their saturation height for unidirectional steady flow and periodic water motion. Furthermore, we consider what happens to the shape and migration rates of sand waves when we allow them to become finite.

First, a description of the case studies is given in Section 2 (for which the results can be found in Section 4). In Section 3, a short description of the simulation model is presented. In Section 4, the results are presented describing the evolution of sand waves using the fully coupled model for a unidirectional steady current, based on data from the Gulf of Cadiz and for periodic water motion representative of North Sea conditions. In the unidirectional steady flow case, we investigate the change in migration rate during the evolution of a sand wave. We investigate the effect of different mechanisms on the results in Section 5.

2. Description case studies

2.1. The North Sea: symmetric sand waves

Large areas of the seabed of the southern bight of the North Sea are covered by sand waves (Stride, 1982; Van Maren, 1998; Hulscher and Van den

Brink, 2001). The water motion in the North Sea is dominated by tidal motion (M_2) (Terwindt, 1971; Van Alphen and Damoiseaux, 1989; Dronkers et al., 1990). Here, we will investigate an area off the Dutch coast (Fig. 1). This area contains sand waves having wavelengths of about 300 m and heights of several meters. The tidal motion (M_2) is of order 1 m/s (Hulscher and Van den Brink, 2001) (Table 1). The grain sizes can vary between 100 and 600 μm (Stolk, 2000; Roos et al., 2004). The results of this case study are discussed in Section 4.2 after the simulation model is discussed in the next section (see also Németh et al., 2004).

2.2. The Gulf of Cadiz: asymmetric sand waves

In the Gulf of Cadiz, sand wave like bed forms in a predominantly unidirectional steady flow are found in average water depths of 20 m on a continental shelf of about 30 km wide (Fig. 2). Due to the nature of the tidal motion in combination with the shape of the coastal environment, the ebb and flood parts of the tidal motion pass over different areas in the Gulf. The wavelengths and heights of the sand waves are typically 150–300 m and 2–4 m, respectively. Both, symmetrical and asymmetrical sand waves are found (see also Rommel, 2002; Németh et al., 2004).

The area of investigation is situated in the Northern part of the shelf (Fig. 2). The area contains relatively small sand waves, having wavelengths between 50 and 350 m with an average of about 145 m. Their heights vary between 1 and 5 m with an average of about 2 m. Their shape is strongly asymmetrical (Table 1). The average grain size is about 537 μm.

The currents in the Gulf of Cadiz are complex. Two main patterns can be identified. The first is a

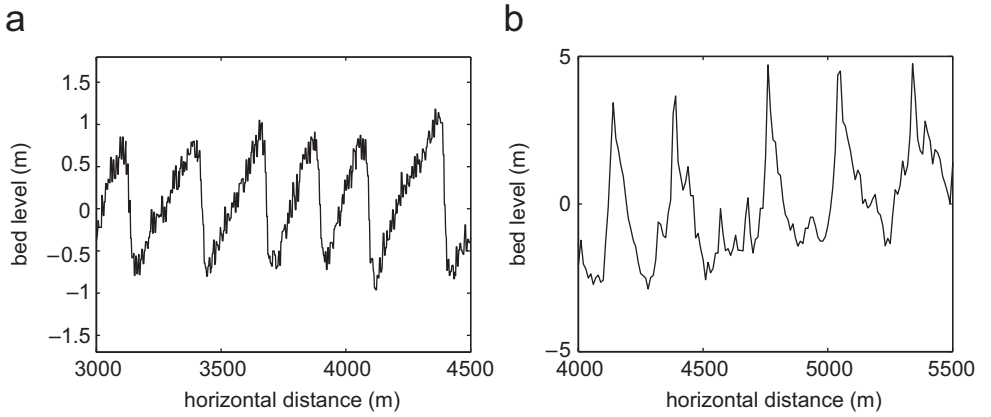

Fig. 1. Sand waves in the North Sea: (a) Shows sand waves off the coast near IJmuiden in the Netherlands. The sand waves are asymmetrical and have a wavelength of about 250 m and a height of maximum 2 m. (b) Shows sand waves at Noord—Hinder in the North Sea, located near the Eurogeul at an average water depth of about 38 m. Their wavelengths are 300 m and their height is typically 6 m. The sand waves are more symmetrical in the horizontal direction and asymmetrical in the vertical with their sharp crests and elongated troughs.

Table 1
Typical values and dimensions of the parameters and variables used in the simulation model

Parameters	Symbol	North Sea	Cadiz	Dimension
Depth-averaged velocity	U	1	0.2	m/s
Average water depth	H	30	22	m
Kinematic eddy viscosity	A_v	5×10^{-3}	2×10^{-2}	m^2/s
Resistance parameter	S	8×10^{-3}	4×10^{-2}	m/s
Gravitational acceleration	g	9.8	9.8	m/s^2
Power of transport	b	5×10^{-1}	5×10^{-1}	—
Proportionality constant	α	3×10^{-1}	3×10^{-1}	s^2/m
Bed slope factor 1	λ_1	6×10^{-3}	2.2×10^{-3}	m^2/s^2
Bed slope factor 2	λ_2	3.33	3.33	—

Fig. 2. Enlargement of study area showing the area used in the Gulf of Cadiz case study located at 36° latitude and 6° longitude. The arrow denotes the current and presumed migration direction of the sand waves. The figure is adapted after Lobo et al. (1999) and Munoz-Perez and Enriquez (1998).

southeast directed inflow of North Atlantic water in the direction of the Mediterranean Sea (Lobo et al., 1999). The second is a north eastward inflow from the Mediterranean sea (Nelson et al., 1999) due to the density contrast between Mediterranean and Atlantic water. This density contrast enforces a reverse estuarine circulation in which the Mediterranean water flows westward along the seabed under the eastward flowing Atlantic water. This distinguishes the area from the North Sea where periodic water motion is dominant and sometimes modified by a steady component.

Therefore, in the Gulf of Cadiz we find offshore sand waves existing in unidirectional and approximately steady flows (see Table 1). The results of this explorative case study are discussed in Section 4.1 after the simulation model is discussed below.

3. Description of the model set up

3.1. 2DV flow model

Since the Coriolis force only slightly affects sand waves (Hulscher, 1996), we limit ourselves to one horizontal direction. After making the shallow water approximation, we obtain the 2DV shallow water equations:

$$\frac{\partial u}{\partial t}+u\frac{\partial u}{\partial x}+w\frac{\partial u}{\partial z}=-g\frac{\partial \zeta}{\partial x}+\frac{\partial}{\partial z}\left(A_v\frac{\partial u}{\partial z}\right), \tag{1}$$

$$\frac{\partial u}{\partial x}+\frac{\partial w}{\partial z}=0. \tag{2}$$

The velocities in the x- and z-directions are u and w, respectively. The water level is denoted by ζ and H represents the mean water depth. The level of the seabed is represented by $z=-H+h$ (Fig. 3). Time is represented by t. The symbols g and A_v indicate the acceleration due to gravity and the vertical eddy viscosity, respectively.

The simulation model is not able to describe flow separation due to the usage of the shallow water approximation. Therefore, for very large sand wave heights, the model is not valid. To describe flow separation the pressure in the domain needs to be taken explicitly into account (Johns et al., 1990; Fredsøe and Deigaard, 1992; Stansby and Zhou, 1998). However, sand waves in an offshore environment in general are not very high and/or steep (vertical change of meters along a horizontal domain of hundreds of meters), due to the more symmetrical water motion instead of the unidirectional *steady* flow found in rivers.

The formulation of the two-dimensional vertical (2DV) numerical simulation model is presented in detail in Németh et al. (2006). The domain of the model is nonperiodic in both directions. The spatial discretization is performed by a spectral method based on Chebyshev polynomials. A fully implicit method is chosen for the discretization in time.

3.2. Sediment transport and seabed behaviour

Bed load transport is the mode of transport presumed dominant in offshore tidal regimes. Suspended sediment transport is not expected to play an important role on the development of sand waves at depths larger than 25 m. Furthermore, Besio and Blondeaux (2003) showed that inclusion of suspended sediment transport does not affect significantly the qualitative behaviour of the system. The following general bed load formula is used following Komarova and Hulscher (2000), modelling bed load transport (S_b) as a function of the shear stress at the seabed (τ_b):

$$S_b=\alpha|\tau_b|^b\left[\tau_b-\lambda_1\frac{\partial h}{\partial x}-\lambda_2|\tau_b|\frac{\partial h}{\partial x}\right], \tag{3}$$

in which:

$$\tau_b=A_v\frac{\partial u}{\partial z}\bigg|_{z=-H+h}, \tag{4}$$

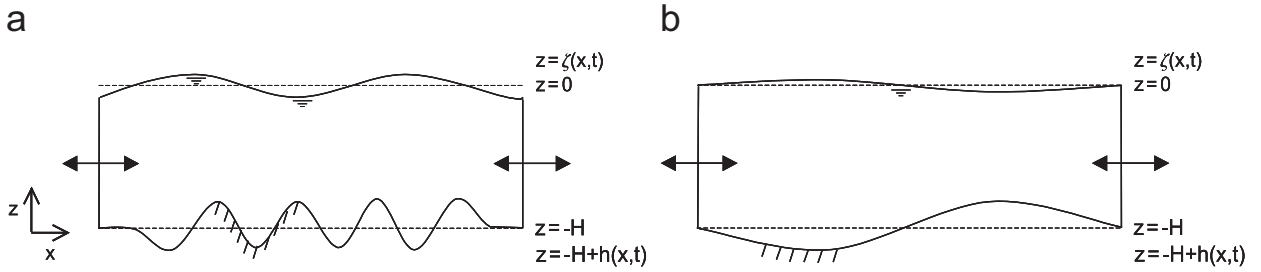

Fig. 3. Definition sketch of the model geometry: (a) Shows the nonperiodic set-up; (b) Shows the usage of periodic boundary conditions. Here, the properties of the variables at the inflow boundary are the same as at the outflow boundary.

and with:

$$\alpha = \frac{8\gamma}{(s-1)g}, \quad \lambda_1 = \frac{3\Theta g(s-1)d}{2\gamma \tan \phi_s}, \quad \lambda_2 = \frac{1}{\tan \phi_s}. \tag{5}$$

Herein, Θ is the critical Shields parameter modelled by a constant of 0.047, s is the relative density of sediment equal to 2.65 and γ accounts for the fact that sediment is not transported when the shear stress is too low. For unidirectional steady flow, this parameter is equal to its maximum 1, otherwise estimated at 0.5 (Komarova and Hulscher, 2000). The grain diameter is denoted by d and ϕ_s is the internal friction angle of the bed with $\tan \phi_s = 0.3$. The power of transport, represented by b, is set at 0.5 and the proportionality constant, denoted by α, is about $0.3\,s^2/m$ and includes the effect of porosity. The scale factors for the bed slope mechanism are λ_1 and λ_2, taking directly into account that sand is transported more easily downhill than uphill (see Table 1).

The sediment balance, which couples the flow model, i.e. Eqs. (1) and (2), with the sediment transport model, i.e. Eq. (3), calculates the seabed level h based on the principle of conservation of mass:

$$\frac{\partial h}{\partial t} = -\frac{\partial S_b}{\partial x}. \tag{6}$$

3.3. Boundary conditions at the free surface and seabed

The hydrodynamic boundary conditions at the water surface ($z = \zeta$) (Fig. 3) are defined as follows:

$$\frac{\partial \zeta}{\partial t} + u\frac{\partial \zeta}{\partial x} = w\Big|_{z=\zeta}, \tag{7}$$

$$\frac{\partial u}{\partial z} = \frac{\tau_w}{A_v}\Big|_{z=\zeta}, \tag{8}$$

in which τ_w describes the wind induced shear stress at the sea surface. The vertical velocity component at the bed ($z = -H + h$) is described by the kinematic condition:

$$\frac{\partial h}{\partial t} + u\frac{\partial h}{\partial x} = w\Big|_{z=-H+h}. \tag{9}$$

The horizontal flow components at the seabed are modelled with the help of a partial slip condition (S is the resistance parameter controlling the resistance at the seabed). This is required due to the usage of a viscosity model with a constant viscosity. The boundary condition couples the resistance at the seabed with the water movement in the direction of the flow:

$$A_v\frac{\partial u}{\partial z} = Su\Big|_{z=-H+h}. \tag{10}$$

3.4. Horizontal boundary conditions

In case of a nonperiodic approach (Fig. 3(a)), an estimate of the water level is supplied to the model at the outflow boundary. Furthermore, the derivatives in the horizontal direction for the horizontal and vertical velocities are set to zero at the outflow boundary.

Here, we investigate the nonlinear behaviour of sand waves with periodic boundary conditions in the horizontal direction (Fig. 3(b)). The values of the variables at the inflow boundary are in this case equal to the values of the variables at the outflow boundary. The physical interpretation of periodic boundary conditions is that we have a train of identical sand waves next to each other.

Using this approach, we choose the length of the domain to be equal to the initially preferred wavelength based on linear theory (see Németh et al., 2002 and Fig. 5). During the morphological calculations this wavelength is fixed. Therefore, the model is not allowed to alter the wavelength of the

sand wave during its evolution. However, this is a common approach. Other related studies into the dynamics of bars in rivers (see Schielen et al., 1993) and shoreface-connected sand ridges (see Calvete et al., 2002) have shown that the initially most preferred mode can play a dominating role in the nonlinear regime.

This assumption is supported by bathymetric data containing offshore sand waves. The data show that the ratio of the height of the sand waves compared to the boundary layer, which is of the order of the water depth, is relatively small (Terwindt, 1971; Van Alphen and Damoiseaux, 1989; Van Maren, 1998; Knaapen et al., 2002; Morelissen et al., 2003). Furthermore, the wavelengths of the linear most preferred modes are similar to the wavelengths observed in the bathymetric data. These characteristics indicate that the system can be not strongly nonlinear, but weakly nonlinear. Therefore, we expect a maximal difference in wavelength (between the initially most preferred mode and the saturated sand wave) of the same order as the expected nonlinearity, which is about 10–20% (the ratio of the sand wave height divided by the water depth or boundary layer thickness) (Dodd et al., 2003 and references herein).

3.5. *Tidal flow simulations using steady and block current*

Two possible origins of steady flow u_r are investigated. These are (I) a wind stress (τ_w) driven current and (II) a current induced by a pressure gradient P. On a plane bed, the vertical structure follows from:

$$\text{I: } u_r = \frac{\tau_w}{A_v}\left(H + \frac{A_v}{S} + z\right), \tag{11}$$

$$\text{II: } u_r = P\left(\frac{1}{2}z^2 - \frac{A_v}{S}H - \frac{1}{2}H^2\right), \tag{12}$$

with P a parameter determining the magnitude of the pressure gradient.

We prescribe the pressure gradient ($\delta\zeta/\delta x$) (time dependent or independent) directly in the momentum equation (Eq. (1)). In this case, no slope will develop in case of a flat bed, since the pressure gradient is present throughout the domain (not only at the inflow boundary). The existence of a net slope in the water level (in the domain) would be inconsistent with the use of periodic boundary conditions. Note, that we still have a free surface. For a flat seabed, the velocity profile in the vertical is in this case equal to Eq. (12) throughout the domain. Prescribing the pressure gradient in this way is equivalent to the basic state in the linear stability analysis in Németh et al. (2002).

While investigating sand waves in the nonlinear regime due to a unidirectional steady current, we will have to deal with sand wave evolution, change in shape and migration. Hereby, we expect the sand wave to become asymmetric. However, if we look at periodic water motion—more typical for offshore locations—the bed forms will not migrate and remain symmetrical in the horizontal. This simplifies the analysis, since the only responses of the system remaining to observe are the evolution of the sand wave and the change in shape (Fig. 6).

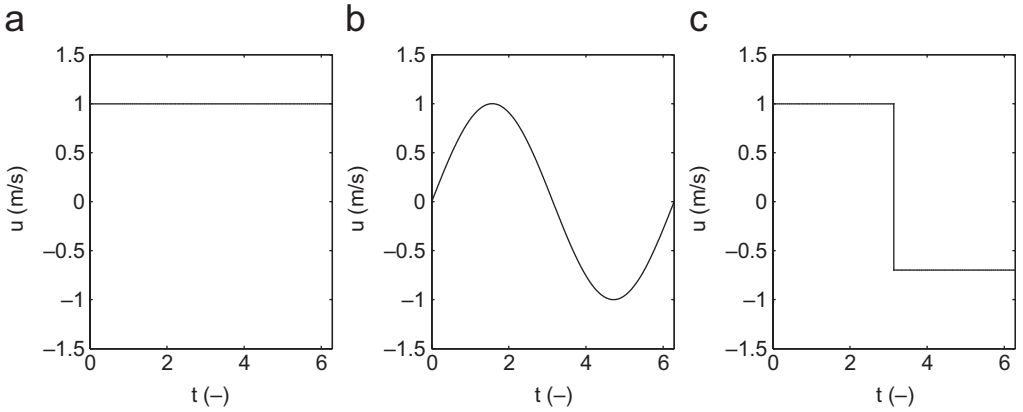

Fig. 4. Various types of water motion: (a) Shows a unidirectional steady current; (b) Shows time-dependent water motion, in this case sinusoidal tidal motion. In (c) a block current can be found, simulating periodic tidal motion, by taking into account two steady currents (a) in opposite direction.

We will simulate tidal motion with a block current. It is based on two steady currents in opposite direction (Fig. 4(a): steady flow and (c): block current). The growth rates for a range of wavelengths for a block current can be found in Fig. 5, indicating the wavelength of the fastest growing mode (about 500 m) is of the same order as for sinusoidal tidal motion (Németh et al., 2002). Furthermore, the numerical effort of investigating tidal motion with a block current is significantly smaller than for sinusoidal tidal motion (Fig. 4(b)). This is especially true when doing long-term morphological calculations.

We investigate two cases: a steady current and a block current simulating tidal motion.

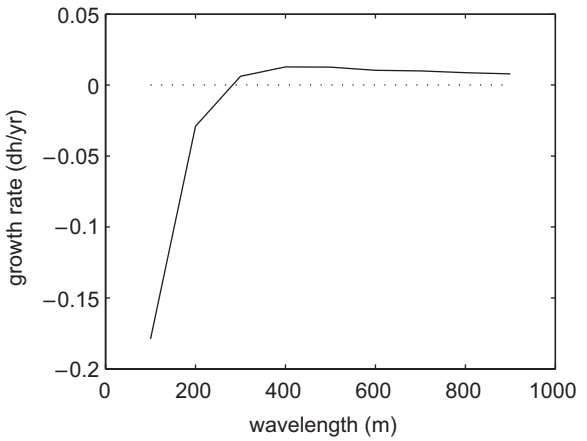

Fig. 5. Growth rate for small amplitude sand waves in a unidirectional block current based on a pressure gradient with a depth-averaged velocity of 1 m/s for a range of wavelengths using the default parameter setting (Table 1).

4. Results

Here, we investigate the evolution of sand waves with the fully coupled simulation model developed in Németh et al. (2006). This means that the changes in the position of the seabed are calculated simultaneously with the water motion.

We start by investigating unidirectional steady flow, with the Gulf of Cadiz as a case study, and then investigate periodic water motion focussing on North Sea conditions.

As nonlinear sand waves are not sinusoidally shaped, we will use the term sand wave height, defined as the distance from the trough to the top (Fig. 6).

4.1. Asymmetric sand waves

Fig. 7 shows the wavelengths of the fastest growing modes according to the linear stability analysis for a range of values of the resistance parameter S and the eddy viscosity A_v in the Gulf of Cadiz. These two variables are considered to be the most difficult to estimate. The rest of the values of the parameters can be found in Table 1. For typical values of the resistance parameter S representing North Sea conditions (see Table 1), we find long wavelengths with unidirectional steady flow only (much longer than the sand waves found in the Gulf of Cadiz). However, for larger values of the roughness at the seabed, we find shorter bed forms (Németh et al., 2001; Idier, 2003). The calculated wavelengths are slightly longer than the actual wavelengths found in the Gulf of Cadiz. Since the

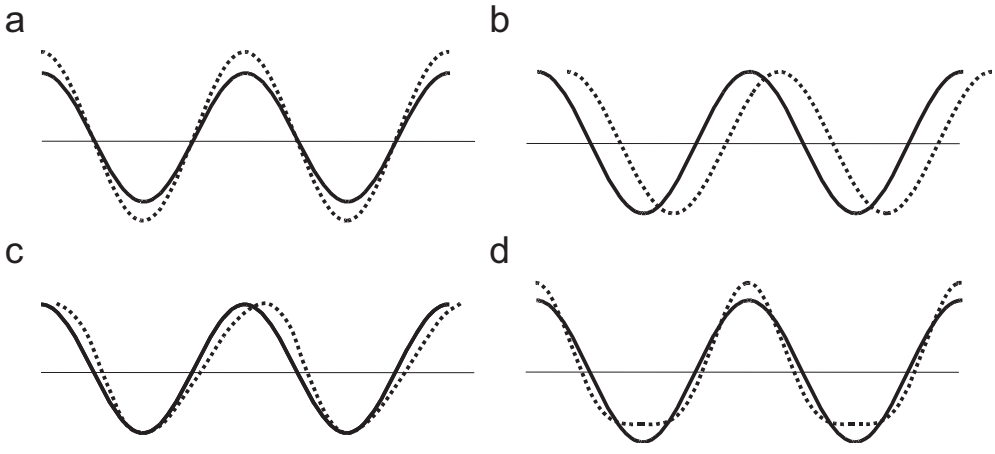

Fig. 6. Possible changes of sand wave profile. The following aspects are shown: (a) growth; (b) migration; (c) change in horizontal asymmetry and (d) change in vertical asymmetry.

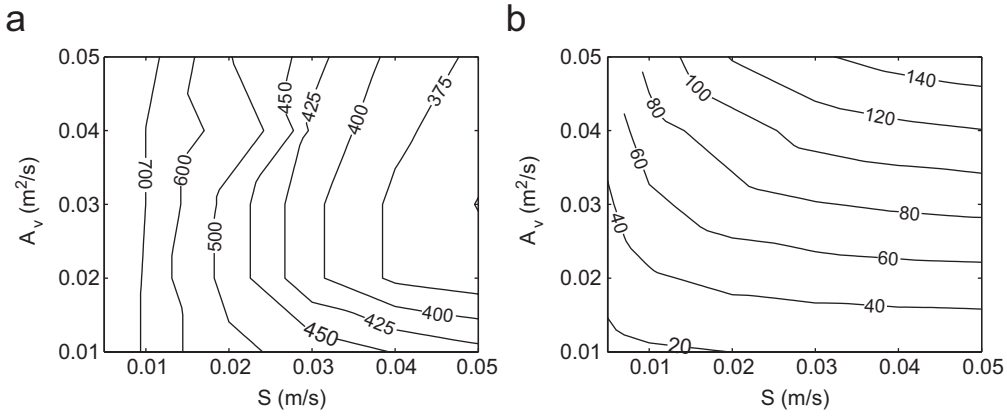

Fig. 7. Properties of the fastest growing mode as a function of S and for different values of A_v for the area investigated in the Gulf of Cadiz: (a) shows the wavelength (m) and (b) the coinciding migration rate (m/yr).

order of magnitude is correct and the available data is limited we conclude that the approach is successful, indicating that bed forms found in the Gulf of Cadiz (Section 2.2) can be modelled as free instabilities of the system. The predicted migration rates could not be verified, since only one measurement was available.

4.1.1. Sand wave evolution

In Figs. 8 and 9(a) the development of the seabed as a function of time is presented. We started with the fastest growing mode determined with the linear stability analysis (Németh et al., 2002) for a steady current induced by a pressure gradient and a value of the resistance parameter S of 0.04 m/s and the eddy viscosity A_v of $0.02\,m^2/s$ (see also Table 1 for the rest of the values of the parameters and Fig. 7).

We can identify the evolution of the sand wave pattern. In Fig. 8(a) the evolution of the crest and trough of the sand wave as a function of time (yr) is shown. The distortion apparent is not a numerical error or higher harmonic in the seabed topography. This virtual distortion is because we plotted the highest and lowest positions of the seabed in the discrete grid points and due to the narrowing grid density near the boundary of the computational domain, where the sand waves pass while migrating. The evolution of the height of the sand wave according to the current model is therefore as smooth as in Fig. 10.

The bed form initially develops slowly, after which the amplitude increases quicker, equivalent to the exponential solution of the linear stability analysis. Next, the growth rate diminishes due to the change in balance between the shear stress at the seabed, transporting sediment upward and the slope term in the sediment transport formula (Eq. (3)) and saturation is found. Based on the parameters used in this study (see Table 1), it takes about 30 years to develop from 10% to 90% of the saturation height of about 5 m. The final height is 22% of the average water depth. These modelled heights and wavelengths of the sand waves lie within the range of the observations. However, they are above average. We should note the slope effect becomes more important for sand waves with smaller wavelengths. Therefore, a smaller wavelength of the fastest growing mode should result into a smaller sand wave height.

The slopes found are still small (the maximum is about 4%). Therefore, no flow separation occurs. This coincides with the observation that the bed forms in this area are more symmetrical than in other areas in the Gulf (see also Lobo et al., 1999). The fully-developed bed pattern is migrating with a migration rate of about 36 m/yr. The cross-section of the fully developed sand wave is shown in Fig. 9(b). However, the asymmetric shape is not yet in equilibrium, and changes further. Sand wave migration is discussed further below.

Similar calculations have been performed for other areas in the Gulf for different values of the resistance parameter S and the eddy viscosity A_v. However, for these investigated cases, containing higher current velocities, the asymmetries of the bed forms become so large during their evolution, that we were not able to describe their entire evolution without flow separation. This is due to the larger

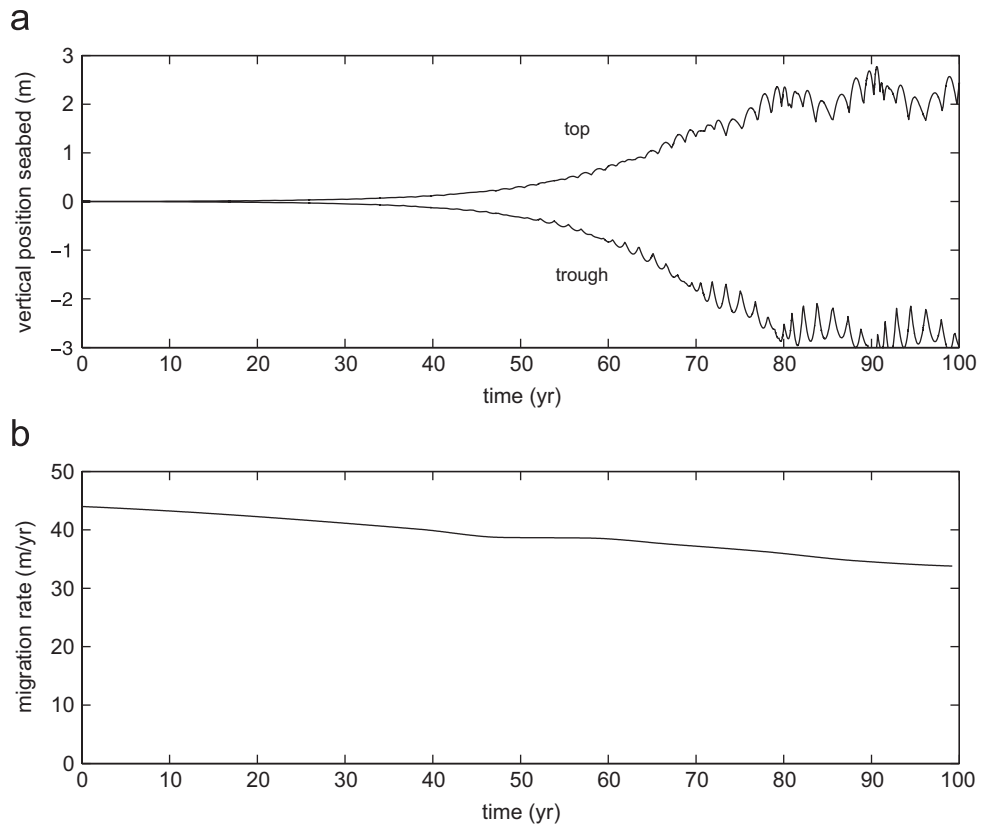

Fig. 8. Evolution and migration of a sand wave in the Gulf of Cadiz. (a) Shows sand wave evolution in a unidirectional steady current using periodic boundary conditions. The upper and lower line represent the evolution as a function of time (yr) of the crest and trough of the sand wave, respectively. The modulations are due to the way of plotting the results and have no physical or numerical reason. (b) Shows the corresponding migration rate during the evolution of the sand wave.

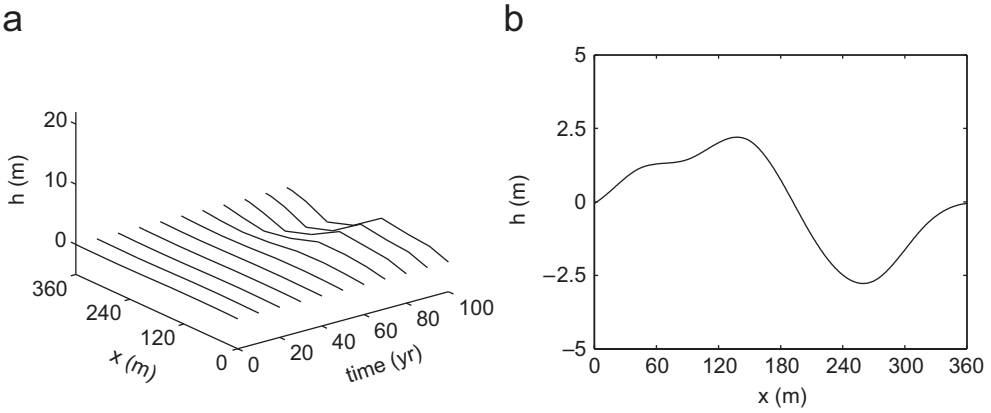

Fig. 9. Cross-section of a sand wave during its evolution in the studied area in the Gulf of Cadiz. (a) Shows the evolution in time of the seabed for a unidirectional steady current. (b) Shows the position of the seabed for the fully-developed sand wave (see also Figs. 1(a) and 6(c)). The position of the bed form has been corrected for its horizontal displacement/migration to make the evolution of the bed form more clear.

shear stresses (due to the higher current velocities). To enable the description of these bed forms, the model needs to be modified as discussed above. The strong asymmetry (in the horizontal) the simulation model predicts coincides with the asymmetry of the sand waves found there.

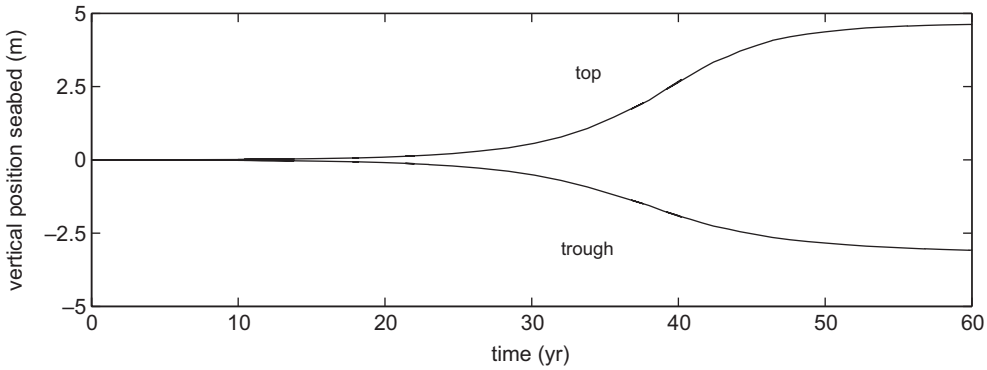

Fig. 10. Sand wave evolution in a block current. The upper and lower line represent the evolution as a function of time (yr) of the crest and trough of the sand wave, respectively. We start the simulation with the fastest growing mode for a resistance parameter of 0.008 m/s and an eddy viscosity of $0.005\,m^2/s$.

4.1.2. Sand wave migration

Fig. 8 shows the evolution of a sand wave in the Gulf of Cadiz as a function of time (see also Table 1). We are interested in the migration rate obtained with the linear stability analysis (Németh et al., 2002) compared with the migration rates for finite amplitudes. The migration rate is defined as the time it takes for the lee side of the sand wave at $z = -H$ to migrate one wavelength. This definition is chosen because we are looking at a steady current, inducing an asymmetric shape not equal to the sinusoidal sand waves investigated with the linear stability analysis. The migration rate decreases slightly, from 44 m/yr for a height of 2 mm to 36 m/yr for the fully-developed sand wave. This means an 18% difference between the result from the linear stability analysis and the fully-grown sand wave, which is not unusual for weakly nonlinear phenomena, in which the deviation from the linear values is of the order of the nonlinearity (here about 20%).

Therefore, the linear stability analysis provides a good estimate of the migration rate, even though the analysis is based on infinitely small sinusoidal sand waves. This can be expected for a weakly nonlinear problem, where the change in sand wave migration should be of the order of the relative sand wave height.

4.2. Symmetric sand waves

Figs. 10 and 11(a) show the evolution of a sand wave for a typical North Sea location (see Section 2.1). A typical value of the resistance parameter S of 0.008 m/s is chosen together with an eddy viscosity A_v of $0.005\,m^2/s$ and an average water depth of 30 m. These values coincide with other values reported in the literature (Hulscher, 1996; Gerkema, 2000; Besio et al., 2004). A comprehensive discussion on these two parameters in relation to observed bed forms can be found in Hulscher and Van den Brink (2001). The value of λ_1 is set at 0.006 and we investigated a block current based on a pressure gradient inducing a depth-averaged velocity of 1 m/s. For the rest of the values of the parameters see Table 1.

We started calculations with a sinusoidal sand wave with a wavelength coinciding with the fastest growing mode. The initial height of the bed form is 0.05 m. The seabed initially develops slowly. However, it takes only 20 years to develop from 10% to 90% of the saturation height. Next, the growth rate of the sand wave diminishes again, due to the increased importance of the slope effect with respect to the uphill directed shear stress for larger heights. The height of the fully-developed sand wave is about 7.8 m, which is 26% of the average water depth. This height lies within the range seen in the North Sea (see also Fig. 1). The water motion still has residual circulation cells oriented toward the crest (Fig. 12). Furthermore, the sand wave does not migrate and shows no asymmetry in the horizontal. It resembles a sinusoidal pattern with a slightly elongated trough.

5. Physical mechanisms

5.1. Slope term

The slope effect is modelled by two separate terms with the parameters λ_1 and λ_2 in Eq. (3) (Komarova

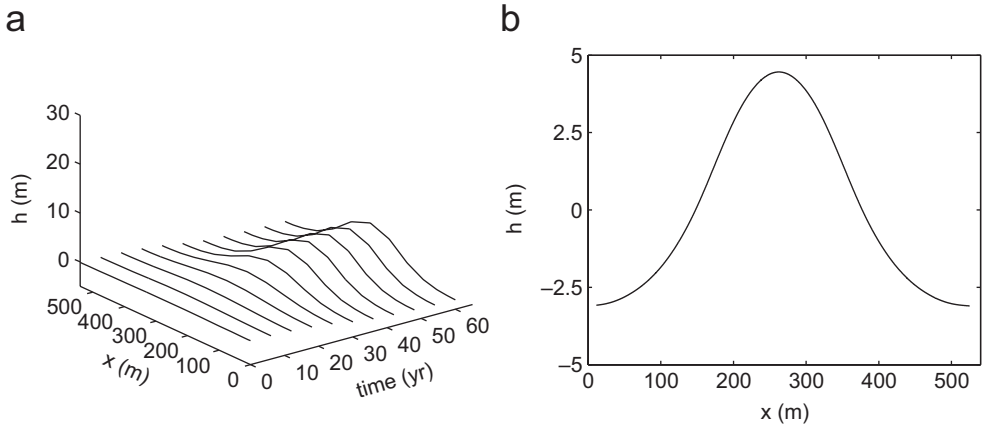

Fig. 11. Cross-section of a sand wave during its evolution and its final shape in the North Sea: (a) shows the evolution in time of the seabed for a block current representing a typical North Sea location; (b) shows the position of the seabed for the fully-developed sand wave.

and Hulscher, 2000). The term containing λ_1 forms the largest contribution to the total slope effect and is equal to (grain weight/area)/(flow shear stress). Furthermore, it is related to the threshold of sediment motion. The second term λ_2 is related to the angle of no repose/friction angle. In a linear analysis (Komarova and Hulscher, 2000; Németh et al., 2002), only the sum of the two terms is important, since the amplitude of the sand waves is small. However, for larger sand wave heights the effects of the different terms become apparent.

Fig. 13(a) shows the profile of a fully-grown sand wave for the typical case calculated for a block current (Table 1 and Figs. 10 and 11). Fig. 13(b) shows the profile using the same value of the slope term for the small amplitude sand wave case, giving the same wavelength for the fastest growing mode, but based on λ_1 ($\lambda_1 = 0.00896$ and $\lambda_2 = 0$). This parameter setting results in a more peaked profile of the sand waves, resembling the pattern found in the North Sea in Fig. 1(b) with more elongated troughs and sharp crests. The height is about the same as in Fig. 13(a). If we set λ_1 to zero and base the slope term for the instability mechanism on λ_2 ($\lambda_1 = 0$ and $\lambda_2 = 10.1$), we obtain Fig. 13(c). In this case, flow separation occurred just before the sand wave reached its larger maximum height of 10 m. For illustrative purposes we plotted this profile to show the smoother shape compared with Fig. 13(a) and (b) due to the different more diffusive character of the slope term containing λ_2 (which can already be identified during the evolution).

Which of the two terms dominate depends on the magnitude of the shear stress and on the magnitude of the slope parameters (Eq. (5)). Based on this analysis, we expect more smooth sand waves for relatively higher shear stresses and peaked sand waves for more moderate conditions.

5.2. Viscosity and resistance at the seabed

We can test the effect of the magnitude of the eddy viscosity A_v and resistance parameter S on the finite amplitude behaviour of sand waves, by varying their values. We calculate, for each combination of S and A_v, the wavelength of the fastest growing mode.

For larger roughness of the seabed, we find shorter wavelengths of the sand waves due to the increased shear stress at the seabed. The growth rate of the sand waves for these larger values of the resistance parameter is larger (see Figs. 14(a)–(c)) due to the combination of the higher shear stress and the shorter wavelengths (smaller volume). The maximum height increases as well (see Fig. 14(b) and (c)). Therefore, the increase in shear stress dominates the increase in slope effect due to the shorter wavelengths. The large resistance at the seabed in Fig. 14(c) caused the flow to separate from the sand wave crest. This effect was enhanced by the sharper gradient in the velocity profile.

Longer fastest growing modes are found for larger values of the eddy viscosity (Németh et al., 2002) (Fig. 15). The rate of evolution increases as well (see Fig. 15(a)–(c)). Starting for the same height of 0.05 m, we find fully-developed sand waves after about 90, 60 and 40 years for values of the eddy viscosity A_v of 0.005, 0.01 and 0.015 m^2/s,

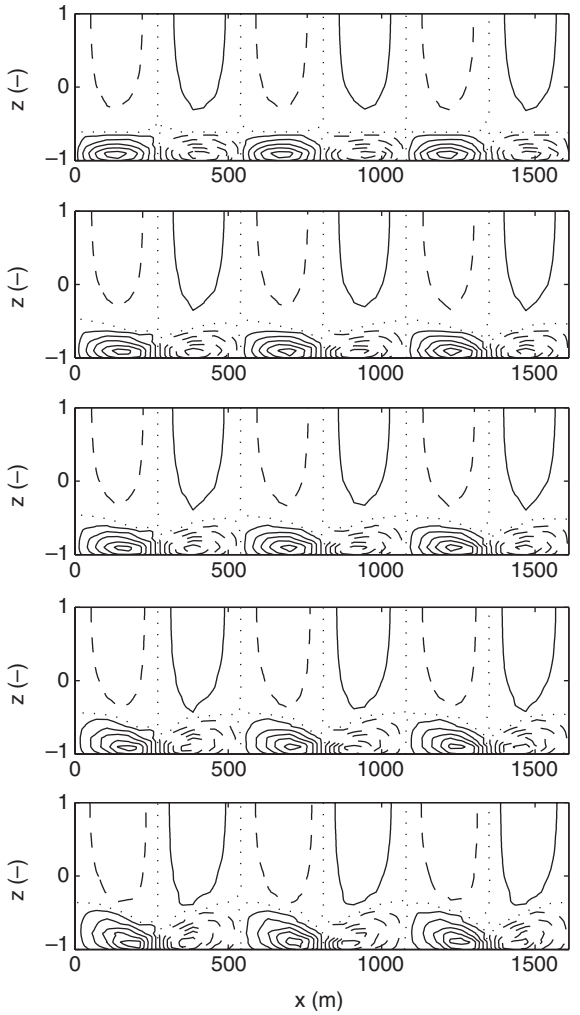

Fig. 12. Contour plot of the horizontal residual current for a block period during the evolution of a sand wave. The sand wave height during its evolution from top to bottom is 0.05, 2, 4, 6, and 7.8 m. The solid lines depict the positive, the dashed lines the negative and the dotted lines a residual flow equal to zero. The position of the water surface and seabed are transferred to $z = 1$ and -1, respectively.

respectively. Furthermore, the maximum height of the sand waves changes almost linearly as a function of the eddy viscosity (see Fig. 15(a)–(c)). This increase in wave height is partly due to the longer fastest growing modes, which have relatively less inhibitions by the slope effect during their evolution.

5.3. Sand wave height and average water depth

Wilkens (1997) investigated with the help of a GIS several characteristics of sand waves and found an almost linear relationship between sand wave height and average water depth (Fig. 16). This linear relationship holds for the range of average water depths in which sand waves are believed to exist (Hulscher and Van den Brink, 2001).

We investigated the effect of the water depth by considering a range of depths. We used the same magnitude of the pressure gradient inducing the water motion for each water depth. The magnitude of the depth-averaged velocity decreases for larger water depths. For each case we calculated the wavelength of the fastest growing mode, which was longer for larger water depths (Fig. 17(a)).

The range of water depths investigated starts at 10 m, where we expect other processes such as suspended sediment and wind waves to play an important role. It ends at 55 m, where according to Fig. 16 the sand waves are small.

With the current parameter settings, flow separation occurs for average water depths less than 25 m. Therefore, the heights shown in Fig. 17 are only indications of the maximum profile of the sand wave in these shallower waters. However, we do not find sand waves of these magnitudes in nature at these water depths. It is possible the parameter settings for this region should be different. Furthermore, aspects such as suspended sediment and wind waves influencing sediment transport are assumed to play an important role in the saturation mechanism under these conditions. These aspects have not yet been incorporated in the model (see also Besio et al., 2003; Calvete et al., 2002).

At larger water depths, we see that the maximum height for a fixed pressure gradient remains about the same. The wavelengths become longer, and the slope term only starts playing a role in the saturation when the heights are large. The relative sand wave height shown in Fig. 17(c) coincides well with Fig. 16(b). However, the absolute heights remain large for larger average water depths. The water depth appears not to encompass the mechanism to explain the absence of sand waves for larger water depths (Fig. 16). However, Fig. 17 coincides better with the idea that the role of the position of the free surface is of lesser importance when the average water depth is of the same order or larger compared to the Stokes layer thickness (the boundary layer). Furthermore, we did not incorporate explicitly a critical shear stress in the sediment transport formulation. The shear stresses can be too low to bring sediment into motion, which could explain the absence of sand waves for larger depths in nature.

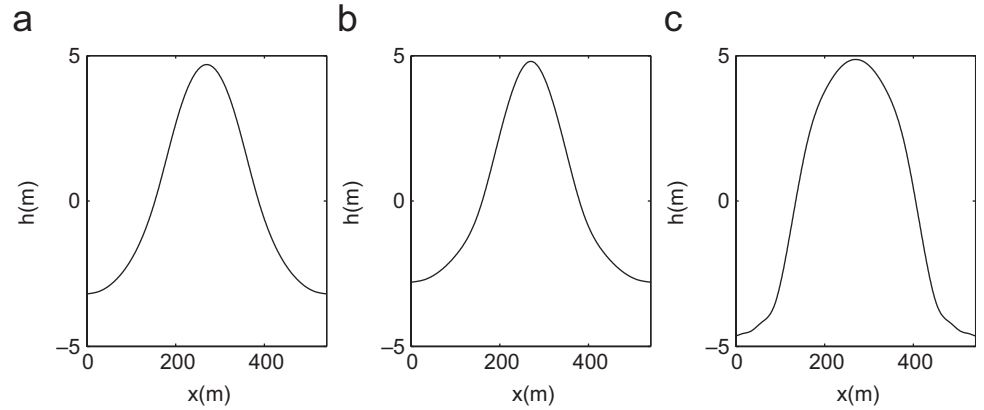

Fig. 13. Influence of the slope term on final cross-section: (a) shows the shape of the fully-developed sand wave induced by a block current for a typical North Sea location with a λ_1 of 0.006 and λ_2 of 3.33; (b) and (c) show fully-developed sand waves for the same conditions except for a λ_1 of 0.00896 and λ_2 of 0 in (b) and λ_1 of 0 and λ_2 of 10.1 in (c). See also Fig. 6(a) and (d).

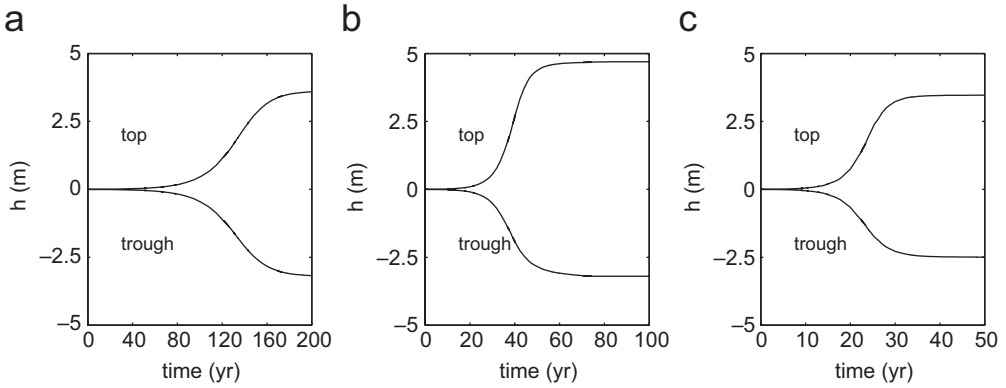

Fig. 14. Influence of the resistance parameter S on sand wave evolution. The three figures show the evolution of the sand wave in time for three values of the resistance parameter S: 0.005, 0.008 and 0.011 m/s. The upper and lower line represent the evolution of the crest and trough of the sand wave, respectively.

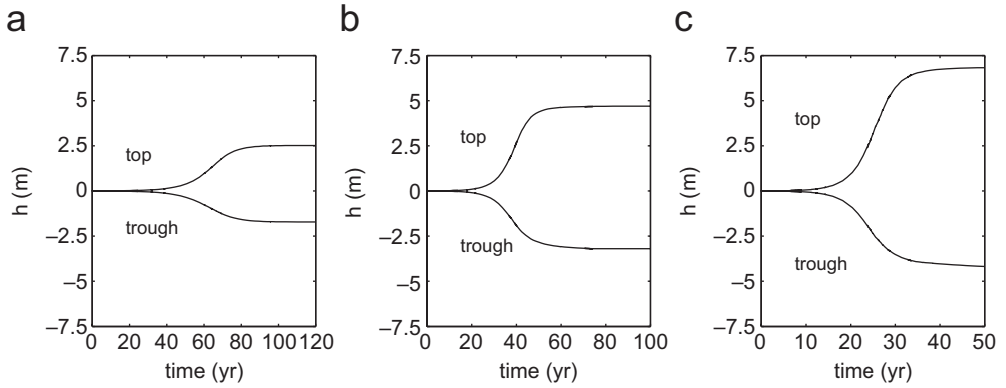

Fig. 15. Influence of the eddy viscosity A_v on sand wave evolution. The three figures show the evolution of the sand wave in time for three values of the eddy viscosity A_v: 0.005, 0.01 and 0.015 m^2/s. The upper and lower line represent the evolution of the crest and trough of the sand wave, respectively.

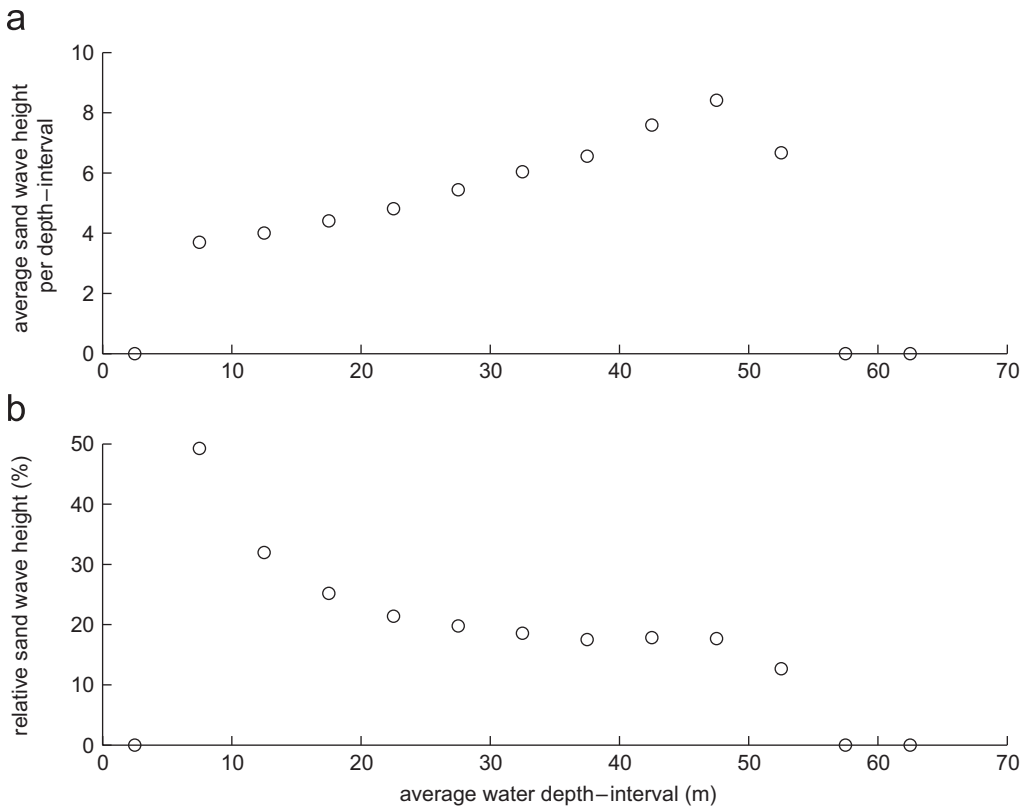

Fig. 16. Measured sand wave height as a function of water depth. (a) Shows the sand wave height (m) distribution over the average water depth (m) as a function of the average sand wave height over a depth-interval (Wilkens, 1997). For small water depths, no sand waves occur since other processes are assumed to become relevant. For large water depths, also no sand waves occur. (b) Shows the relative sand wave height (m) over the average water depth (m) (height/average water depth) as a function of the average sand wave height over a depth-interval.

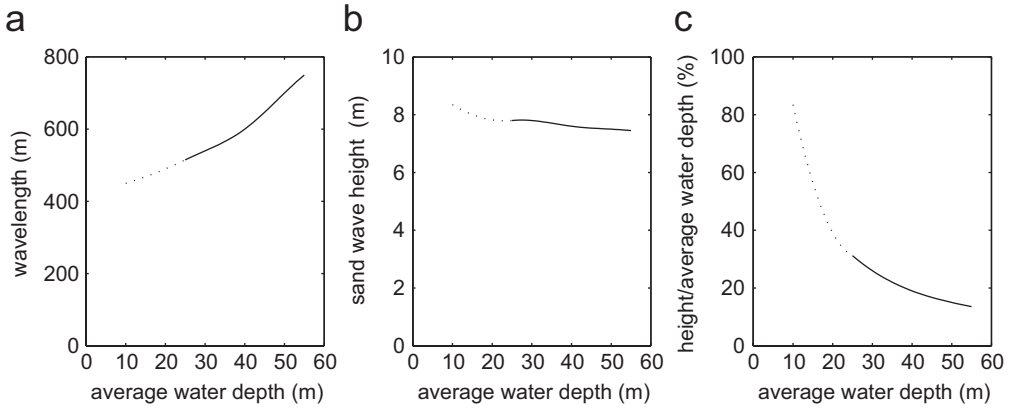

Fig. 17. Calculated sand wave height as a function of water depth: (a) shows the wavelength (m) of the fastest growing mode for a range of water depths, based on a block current; (b) shows the maximum sand wave height calculated; (c) shows the relative sand wave height ((*height*/*averagewaterdepth*) $*$ 100%). For average water depths less than 25 m, we encountered flow separation for this parameter setting (dotted part).

6. Discussion and conclusions

With the numerical model developed herein, we are able to allow a sand wave to evolve to a maximum, saturated height. The simulated sand waves reach heights of 10–30% of the average water depth. It takes about 20 years to evolve from 10% to 90% of the saturation height. This coincides with

values reported in the literature (Knaapen and Hulscher, 2002; Idier, 2003) and with the cases discussed in this paper.

The stabilization mechanism found here causing sand waves to saturate is based on the balance between the shear stress at the seabed and the fact that sediment is transported easier downhill than uphill. The shear stress is a function of the resistance at the seabed and the eddy viscosity. The water motion has residual circulation cells oriented toward the crest for periodic water motion for infinitely small as well as fully-developed sand waves. At larger heights, the slope term reduces the net amount of sediment transported upward toward the crest, which causes the sand wave to saturate.

The steepness found for fully-developed sand waves is less for periodic water motion than for sand waves in steady flow. In the latter case, sand waves can evolve without flow separation when flow conditions are moderate. For less moderate flow conditions, the sand waves become too asymmetrical during their evolution and require the description of flow separation processes to describe their entire evolution. This coincides with observations made by Belderson and Stride (1969), describing a correlation between the direction of sand wave asymmetry and the tidal current asymmetry (see also Fig. 1).

Furthermore, the migration rate becomes only slightly smaller during the evolution from an infinitely small to a fully-grown sand wave. This allows us to use the linear stability analysis to obtain an estimate of the migration rate of sand waves.

The resistance at the seabed and the viscosity are important factors determining the value of the shear stress at the seabed. Therefore, they play an important part in the balance between the shear stress and the slope term in the sediment transport formula. Larger resistance at the seabed and larger values of the eddy viscosity decrease the timescales and increase the saturation heights. The viscosity model used is simple, but it is assumed to be adequate until the relative amplitude of sand waves. The latter is about 20% of the water depth.

For periodic water motion, the balance between the shear stress at the seabed and the slope term determines not only the height but also the shape of the sand wave. When the λ_1 component of the slope term is larger than the λ_2 component, the sand wave tends to be more sharp-crested.

The water depth plays an important role determining the wavelength of the fastest growing mode. Therefore, the saturation height is correlated to the average water depth, since it indirectly effects the influence of the slope effect on the sand wave saturation. However, when the ratio of the average water depth divided by the Stokes layer is larger, the relative effect becomes smaller.

Lastly, when no bathymetric data are available, the results obtained with the sand wave evolution model can be used as an estimate to derive estimates of the parameters necessary for the data assimilation models developed by Knaapen and Hulscher (2002) and Morelissen et al. (2003).

Acknowledgements

This work is supported by Technology Foundation STW, the applied science division of NWO and the technology programme of the Ministry of Economic Affairs and performed within the EU-sponsored project HUMOR (HUman interaction with large-scale coastal MORphologic evolution; EVK3-CT-2000-00037).

References

Belderson, R.H., Stride, A.H., 1969. Tidal currents and sand wave profiles in the north-eastern Irish Sea. Nature 222, 74–75.

Besio, G., Blondeaux, P., 2003. On the effect of the suspended load on the formation of sand waves. Third IAHR Symposium on River, Coastal and Estuarine Morphodynamics, RCEM 2003, vol. I, Barcelona, Spain, pp. 365–375.

Besio, G., Blondeaux, P., Brocchini, M., Vittori, G., 2003. Migrating sand waves. Ocean Dynamics 53, 232–238.

Besio, G., Blondeaux, P., Brocchini, M., Vittori, G., 2004. On the modeling of sand wave migration. Journal of Geophysical Research 109, C04018.

Calvete, D., De Swart, H.E., Falqués, A., 2002. Effect of depth-dependent stirring on the final amplitude of shoreface-connected sand ridges. Continental Shelf Research 22 (18–19), 2763–2776.

Dodd, N., Blondeaux, P., Calvete, D., de Swart, H.E., Falques, A., Hulscher, S.J.M.H., Rozynski, G., Vittori, G., 2003. The role of stability methods for understanding the morphodynamic behaviour of coastal systems. Journal of Coastal Research 19 (4), 849–865.

Dronkers, J., Van Alphen, J.S.L.J., Borst, J.C., 1990. Suspended sediment transport processes in the Southern North Sea. Coastal and Estuarine Studies 38, 302–320.

Fredsøe, J., Deigaard, R., 1992. Mechanics of Coastal Sediment Transport. Institute of Hydrodynamics and Hydraulic Engineering, Technical University of Denmark, Denmark, pp. 260–289.

Gerkema, T., 2000. A linear stability analysis of tidally generated sand waves. Journal of Fluid Mechanics 417, 303–322.

Hansen, E.A., 1989. Migration rate minimum and equilibrium heigth of moving sand dunes. Institute of Hydrodynamics and

Hydraulic Engineering, Progress Report 69, Technical University of Denmark, pp. 39–46.
Hulscher, S.J.M.H., 1996. Tidal induced large-scale regular bed form patterns in a three-dimensional shallow water model. Journal of Geophysical Research 101 (C9), 20727–20744.
Hulscher, S.J.M.H., Dohmen-Janssen, C.M., 2005. Introduction to special selection on marine sandwaves and river dune dynamics. Journal of Geophysical Research 110, F04S01.
Hulscher, S.J.M.H., Van den Brink, G.M., 2001. Comparison between predicted and observed sand waves and sandbanks in the North Sea. Journal of Geophysical Research 106 (C5), 9327–9338.
Huthnance, J., 1982a. On one mechanism forming linear sandbanks. Estuarine, Coastal Shelf Science 14, 79–99.
Huthnance, J., 1982b. On the formation of sand banks of finite extent. Estuarine, Coastal Shelf Science 15, 277–299.
Idier, D., 2003. Dynamique des bancs et des dunes de sable du plateau continental. Observations in-situ et modélisation numérique. Ph.D. Thesis, L'institut national polytechnique de Toulouse, France.
Johns, B., Soulsby, R.L., Chesher, T.J., 1990. The modelling of sand wave evolution resulting from suspended and bed load transport of sediment. Journal of Hydraulic Research 28 (3), 355–374.
Knaapen, M.A.F., Hulscher, S.J.M.H., 2002. Regeneration of dredged sand waves. Coastal Engineering 46 (4), 277–289.
Knaapen, M.A.F., Hulscher, S.J.M.H., De Vriend, H.J., Stolk, A., 2002. A new type of bedwaves. Geophysical Research Letters 28 (7), 1323–1326.
Komarova, N.L., Hulscher, S.J.M.H., 2000. Linear instability mechanisms for sand wave formation. Journal of Fluid Mechanics 413, 219–246.
Komarova, N.L., Newell, A.C., 2000. Non-linear dynamics of sandbanks and sand waves. Journal of Fluid Mechanics 415, 285–321.
Lobo, F.J., Hernandez-Molina, F.J., Somoza, L., Rodero, J., Maldonado, A., Barnolas, A., 1999. Patterns of bottom current flow deduced from dune asymmetries over the Gulf of Cadiz shelf (southwest Spain). Marine Geology 164, 91–117.
Morelissen, R., Hulscher, S.J.M.H., Knaapen, M.A.F., Németh, A.A., Bijker, R., 2003. Interacting sand waves and pipelines: a data-assimilation based mathematical model. Coastal Engineering 48 (3), 197–209.
Munoz-Perez, J.J., Enriquez, J., 1998. Litoral dynamic of a complete physiography unit: Sanlucar-Rota. Revista de Obras Publicas 3375, 35–44.
Nelson, C.H., Baraza, J., Maldonado, A., Rodero, J., Escutia, C., Barber, J.R., 1999. Influence of the Atlantic inflow and Mediterranean outflow currents on Late Quaternary sedimentary facies of the Gulf of Cadiz continental margin. Marine Geology 155, 99–129.
Németh, A.A., Hulscher, S.J.M.H., van Damme, R.M.J., 2001. Numerical simulation of sand wave evolution in shallow shelf seas. In: Hanson, H., Larson, M. (Eds.), Coastal Dynamics. Lund, Sweden, pp. 1048–1057.
Németh, A.A., Hulscher, S.J.M.H., de Vriend, H.J., 2002. Modelling sand wave migration in shallow shelf seas. Continental Shelf Research 22 (18–19), 2795–2806.
Németh, A.A., Hulscher, S.J.M.H., de Vriend, H.J., 2003. Offshore sand wave dynamics engineering problems and future solutions. Pipeline and Gas Journal 230 (4), 67–69.
Németh, A.A., Hulscher, S.J.M.H., van Damme, R.M.J., 2004. Modelling sand wave migration and height, comparing model results with data. In: Hulscher, S., Garlan, T., Idier, D. (Eds.), Marine Sandwave and River Dune Dynamics II, International Workshop, April 1–2, 2004, University of Twente, The Netherlands, pp. 232–239.
Németh, A.A., Hulscher, S.J.M.H., van Damme, R.M.J., 2006. Simulating offshore sand waves. Coastal Engineering, 265–275, doi:10.1016/j.coastaleng.2005.10.014.
Richards, K.J., Taylor, P.A., 1981. A numerical model of flow over sand waves in water of finite depth. Geophysical Journal of the Royal Astronomical Society 65, 103–128.
Rommel, M.C., 2002. Sand wave migration in the Gulf of Cadiz: prediction from a model limit situation. M.Sc. Thesis, University of Twente, The Netherlands.
Roos, P.C., Hulscher, S.J.M.H., Knaapen, M.A.F., Van Damme, R.M.J., 2004. The cross-sectional shape of tidal sandbanks: modeling and observations. Journal of Geophysical Research 109, F02003.
Schielen, R., Doelman, A., De Swart, H.E., 1993. On the nonlinear dynamics of free bars in straight channels. Journal of Fluid Mechanics 252, 325–356.
Stansby, P.K., Zhou, J.G., 1998. Shallow water flow solver with non-hydrostatic pressure: 2D vertical plane problems. International Journal for Numerical Methods in Fluids 28 (3), 541–563.
Stolk, A., 2000. Variation of sedimentary structures and grainsize over sandwaves, In: Trentesaux, A., Garlan, T. (Eds.), Marine Sandwave Dynamics, International Workshop, March 23–24, 2000, University of Lille, France, pp. 193–197.
Stride, A.H., 1982. Offshore Tidal Sands Offshore Tidal Sands: Processes and Deposits. Chapman & Hall Ltd., London, New York.
Terwindt, J.H.J., 1971. Sand waves in the southern bight of the North Sea. Marine Geology 10, 51–67.
Van Alphen, J.S.L.J., Damoiseaux, M.A., 1989. A geomorphological map of the Dutch shoreface and adjacent part of the continental shelf. Geologie en Mijnbouw 68, 433–444.
Van Maren, D.S., 1998. Sand Waves, A State-of-the-art Review and Bibliography, North Sea Directorate, Ministry of Transport, Public Works and Water Management, The Netherlands.
Wilkens, J., 1997. Sand waves and possibly related characteristics. Report for Alkyon Hydraulic Consultancy and Research, The Netherlands.